Front. Mater. Sci. 2014, 8(4): 343–353
DOI 10.1007/s11706-014-0264-6

RESEARCH ARTICLE

In vitro degradation of MAO/PLA coating on Mg–1.21Li–1.12Ca–1.0Y alloy

Rong-Chang ZENG (✉)[1,2], Wei-Chen QI[1,2], Ying-Wei SONG[3], Qin-Kun HE[1], Hong-Zhi CUI[1], and En-Hou HAN[3]

1 College of Materials Science and Engineering, Shandong University of Science and Technology, Qingdao 266590, China
2 State Key Laboratory of Mining Disaster Prevention and Control Co-founded by Shandong Province and the Ministry of Science and Technology, Shandong University of Science and Technology, Qingdao 266590, China
3 National Engineering Center for Corrosion Control, Institute of Metals Research, Chinese Academy of Sciences, Shenyang 110016, China

ABSTRACT: Magnesium and its alloys are promising biomaterials due to their biocompatibility and osteoinduction. The plasticity and corrosion resistance of commercial magnesium alloys cannot meet the requirements for degradable biomaterials completely at present. Particularly, the alkalinity in the microenvironment surrounding the implants, resulting from the degradation, arouses a major concern. Micro-arc oxidation (MAO) and poly(lactic acid) (PLA) composite (MAO/PLA) coating on biomedical Mg–1.21Li–1.12Ca–1.0Y alloy was prepared to manipulate the pH variation in an appropriate range. Surface morphologies were discerned using SEM and EMPA. And corrosion resistance was evaluated via electrochemical polarization and impedance and hydrogen volumetric method. The results demonstrated that the MAO coating predominantly consisted of MgO, Mg_2SiO_4 and Y_2O_3. The composite coating markedly improved the corrosion resistance of the alloy. The rise in solution pH for the MAO/PLA coating was tailored to a favorable range of 7.5–7.8. The neutralization caused by the alkalinity of MAO and Mg substrate and acidification of PLA was probed. The result designates that MAO/PLA composite coating on Mg–1.21Li–1.12Ca–1.0Y alloys may be a promising biomedical coating.

KEYWORDS: magnesium alloy; micro-arc oxidation (MAO); poly(lactic acid) (PLA); biomaterial; degradation

Contents

Received July 20, 2014; accepted September 7, 2014

E-mail: rczeng@foxmail.com

1 Introduction

In recent decades, the most metallic bone implants for clinic applications are stainless steels and titanium alloys which are non-biodegradable [1]. Since the metallic implant is a foreign body to human tissues, the risk of adverse effects or local inflammation may increase after a long-term implantation. In this case, the second surgery is necessary to remove the implants. However, the repeated surgery improves the morbidity rate of the patients and results in an increase in hospitalization cost and time. The applications of biodegradable metallic implants may reduce such complications [2–4].

To serve as the orthopaedic implants, one desirable demand of biomedical materials is their biodegradability [5]. Magnesium and its alloys are the most suitable metal among all the metallic materials. The first study of the application of magnesium alloys as medical implant materials has been recorded early in the last century [6]. However, the major obstacles of magnesium alloys in clinical applications are the lower corrosion resistance and higher hydrogen release rate as well as the rapid alkalinity of solution. Therefore, the corrosion rate of magnesium alloys must be accommodated to the request of implantation [7].

Usually, the corrosion resistance of magnesium alloys can be enhanced by alloying with the elements such as Zn, Ca, Li, and rare earth elements (REs) as well [8–12], and surface modification [13]. Ca is a major component of human bone, which may refine the grains in the microstructure and improve the strength of Mg alloys [14].

The addition of Li can reduce the *c*/*a* ratio of the hexagonal closed packed (HCP) structure of magnesium, cause better malleability and impact resistance [15]. Our previous study shows that Mg–Li–Ca alloys have both corrosion resistance and mechanical properties superior to Mg–Ca alloys [16–17]. For example, LAE442 served as degradable bone lamellas and cardiovascular stents with suitable biomechanical properties [18].

Yttrium also leads to the refinement in microstructure, the improvement in plasticity and tensile strength, and corrosion resistance of Mg alloys [18–19]. Meanwhile, the oxide Y_2O_3 in the naturally formed oxide film on magnesium–yttrium alloy possesses a favorable Pilling–Bedworth ratio (PBR) of 1.13. Therefore, the Mg–Li–Ca–Y alloy is expected to exhibit a good ductility and corrosion resistance.

However, the alloying of magnesium alloys cannot completely satisfy the clinical demand. Surface modification, i.e., micro-arc oxidation (MAO) coating [20–21], chemical conversion coating [22] and polymeric coating [23], can further improve the corrosion resistance and biocompatibility of magnesium alloys [24]. Particularly, the MAO coating, with high hardness, adhesion to the substrate and superior corrosion resistance, gets a wide application.

Nevertheless, MAO can be prone to be attacked by the electrolyte containing Cl^- ions because of the porous surface. MAO coating is comprised of ceramic phases such as magnesium oxide. When these ceramic phases hydrolyzed *in vivo*, local pH value would be raised to a detrimental level to tissues [25]. Thus, MAO coating would be not suitable for replacement implants without sealing or post treatment.

The degradable polymeric coatings, containing poly (lactic acid) (PLA), poly(ε-caprolactone) (PCL) [23,26] and poly(glycolic acid) (PGA) [27], can reduce the corrosion rate and meet the clinical requirement, concerning the biomedical application of magnesium alloys. The *in-vitro* studies on the polymeric coating, fabricated by PCL and dichloromethane onto magnesium alloys, indicated its good cytocompatibility [28]. It is demonstrated that PCL coating on the AZ31 and Mg4Y alloys provides better protection at the initial stage. Nevertheless, it does not maintain a reduction in corrosion rate in the subsequent immersion [29]. This scenario is attributed to the pure polymeric coating peeling from the substrate.

Generally, polymeric coating swells in aqueous solution and thus detaches from the substrates. As the polymer coating fractured locally, galvanic corrosion would occur between the substrate and its coating, and thus accelerated the corrosion. Accordingly, bonding force between the polymer layer and its substrate explicitly influences *in vivo* service time of the coating [21].

Interestingly, the polymeric coating prepared on the porous MAO coating, leading to an interlocking MAO/PLA composite coating, reduces the corrosion rate of magnesium alloys [30–31]. In the composite coating polymer permeates into the porous MAO coating and protects it from the attack by electrolyte ions. Hereby, the porous structure of MAO coating provides a favorable

bond in long-term immersion test.

Nevertheless, it is noted that the decrease in solution pH ascribed to the degradation of PLA is rarely discussed in the literature [26]. The alkalization caused by the corrosion of magnesium and the acidification by the degradation of PLA might tailor the local pH in the microenvironment of the implanted location. Thus, fabricating a PLA coating on the MAO coating may be a promising approach to reducing the corrosion resistance, manipulating the pH at an appropriate level and improving the biocompatibility of magnesium alloys.

The study aims to fabricate a PLA/MAO composite coating, and to have further insight into the degradation mechanism of the MAO/PLA composite coating on Mg–Li–Ca–Y alloy.

2 Materials and methods

2.1 Materials

Mg–Li–Ca–Y alloy was supplied by Institute of Metals Research, Chinese Academy of Sciences (Shenyang, China). The chemical composition of the alloy was 1.21 wt.% Li, 1.21 wt.% Ca, 1.0 wt.% Y, and balance Mg.

The samples for tests was machined to the dimensions of 20 mm × 20 mm × 5 mm. Prior to the preparation of the coating, the samples were ground to 2400 grit, degreased in ethanol, rinsed in de-ionized water and dried in warm air.

2.2 Preparation of coating

The MAO treatment device consisted of a pure titanium plate served as the cathode, a power supply unit controlled by single chip micyoco (SCM) and a stirring/cooling system. The MAO procedures were conducted in a silicate electrolyte, containing 20 g/L NaOH, 20 g/L Na_2SiO_3, 15 g/L NaB_4O_7 and 10 g/L $C_6H_5Na_3O_7$ and 7.5 g/L phytic acid as well [32]. The MAO coating was treated at a constant voltage of 130–140 V for 10 min at room temperature. All solutions used in the process were prepared with A.R. chemicals and distilled water.

In practice, the degradation rate of PLA/MAO composite coating can be adjusted by changing PLA concentration in dichloromethane [23,26]. A low concentration of PLA was chosen to accelerate the degradation rate, since complete degradation time of PLA depends on its molecular weight [33]. To prepare the PLA coating on the MAO surface, PLA with a molecular weight of 60,000 and dichloromethane were firstly mixed in a concentration of 1% (w/v), and then stirred at room temperature for 1 h and dispersed in ultrasonic for 15 min. The samples with the MAO coating were dipped in the mixed solution of PLA and dichloromethane under ultrasonic vibration for 15 min, and then taken out, finally dried in a dry furnace at 65°C for 10 h to make the organic solvent evaporate completely.

Similarly, PLA coating was prepared on a plate of polytetrafluoroethylene (PTFE) in order to investigate the influence of PLA on solution pH during degradation.

2.3 Surface analysis

Scanning electron microscopy (SEM, KYKY-2800B) was employed to discern the surface morphology of the MAO/PLA coating and the corrosion morphologies after immersion in Hank's solution for 72 h. The average pore size and the total pore area were analyzed using Image-PRO plus program (Media Cybernetics Company, USA). The elemental distribution of the composite coating was analyzed by electron microprobe analysis (EMPA, JXA-8230). The structure of MAO coating and MAO/PLA coating soaked in Hank's solution for 72 h were probed by X-ray diffraction (XRD, D/Max2500PC).

2.4 Electrochemical measurement

An electrochemical workstation (PARSTAT 2273) connected to a three-electrode cell was used for the electrochemical measurements. The working electrode was the test material with an exposed area of 1.00 cm^2. A pure platinum electrode and a saturated calomel electrode (SCE) were used as the counter and reference electrodes, respectively. The electrolytic solution was Hank's solution at a pH of 7.4 and room temperature (25°C). At the beginning of electrochemical measurements, the samples were held in the Hank's solution for 15 min to establish the surface steady state. Potentiodynamic polarization curves derived at a sweep rate of 1 mV/s. In electrochemical impedance spectroscopy (EIS) measurements, the frequency ranged from 100 kHz to 10 MHz and the amplitude of the sinusoidal potential signal was 10 mV. The repeated measurements were performed to ensure reproducibility of the results.

2.5 Hydrogen evolution and pH monitor

The hydrogen evolution rate (HER) and pH value were measured to evaluate the corrosion behavior of the

substrate and its coatings during immersion in Hank's solution at 37.5°C. The ratio of the sample-surface-area to medium-volume was 40 mL to 1 cm^2. The method for HER is reported in our previous literature [17]. A pH meter (Alalis pH400) was used to monitor the variation in solution pH value. The solution was not changed during the whole immersion test. All tests were repeated in triplicate.

3 Results

3.1 Morphology observation

The MAO coating on Mg–1.21Li–1.12Ca–1.0Y alloy has a variety of pores and cracks (Fig. 1(a)). The "crater-like" pores are the results of plasma discharges. The number and size of the pores of the MAO/PLA coating markedly reduced (Table 1 and Fig. 1(b)).

Moreover, a stratified structure was easily observed in cross-section (Fig. 2). The MAO coating consist of two clearly pronounced sublayers: a denser inner sublayer or barrier layer and a loose porous outer sublayer. The PLA coating with a bright layer in the outmost layer has several-micrometer thickness. The cracks existed between the PLA coating and epoxy resin because of their different contraction rates as the resin cured. It is noting that considerable microvoids exist in the PLA coating.

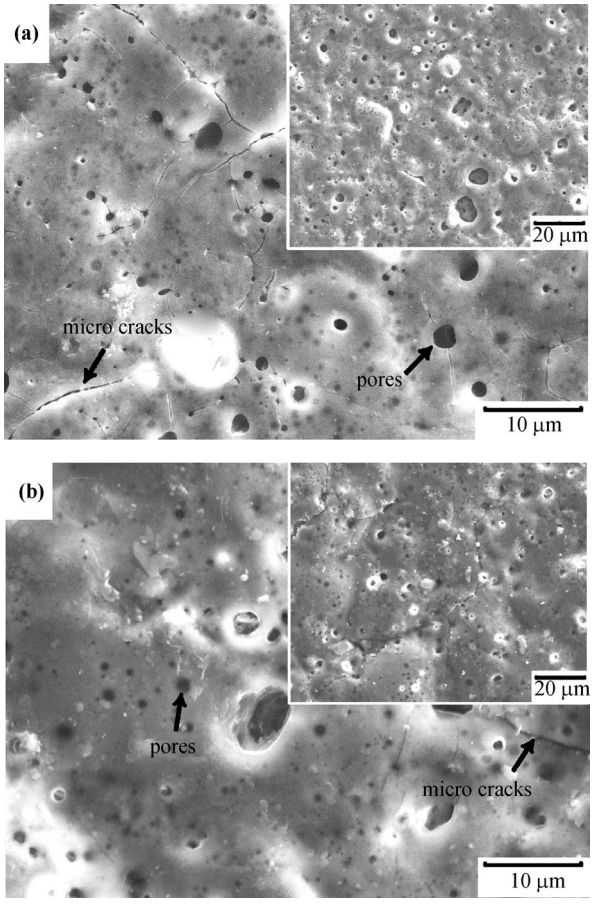

Fig. 1 SEM images of **(a)** MAO coating and **(b)** MAO/PLA coating on Mg–1.21Li–1.12Ca–1.0Y alloy.

3.2 Surface elements analysis

The elemental distribution mapping of the MAO coating (Fig. 3) demonstrates the element enrichment and removal because of high temperature during MAO process [34]. Mg and Ca were predominantly distributed in the substrate, the barrier layer of the MAO coating [35]; while O and Si were completely scattered in the MAO coating; and trace of P, originating from phytic acid, was also found in the MAO coating. These elements indicated the possible existence of MgO, Mg_2SiO_4, and some calcium phosphates such as $CaHPO_4$ and/or $Ca_3(PO_4)_2$ [21] in the MAO coating.

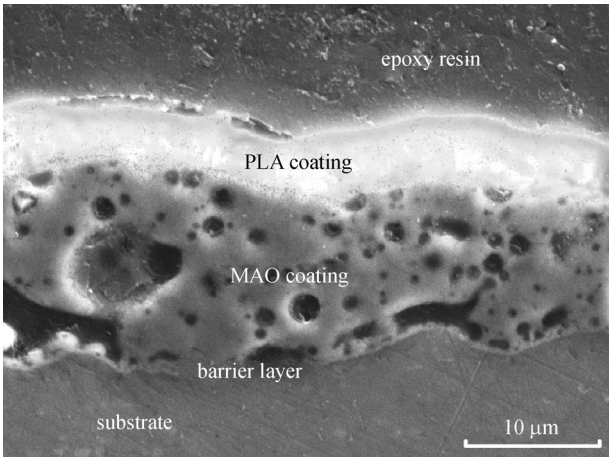

Fig. 2 SEM image of the MAO/PLA coating on cross-sectional view.

3.3 Electrochemical measurements

The both coatings, with lower one order of magnitude of current densities than the substrate, indicate the effective

Table 1 Pore size of the coatings on Mg–1.21Li–1.12Ca–1.0Y alloy

Sample	d_{max} [a] /μm	d_{min} [b] /μm	d_{mean} [c] /μm	Standard deviation	Number of pores
MAO	60.56	~1	8.61	18.81	15332
MAO/PLA	31.42	~1	2.26	2.58	3489

a) The maximum diameter. b) The minimum diameter. c) The mean diameter.

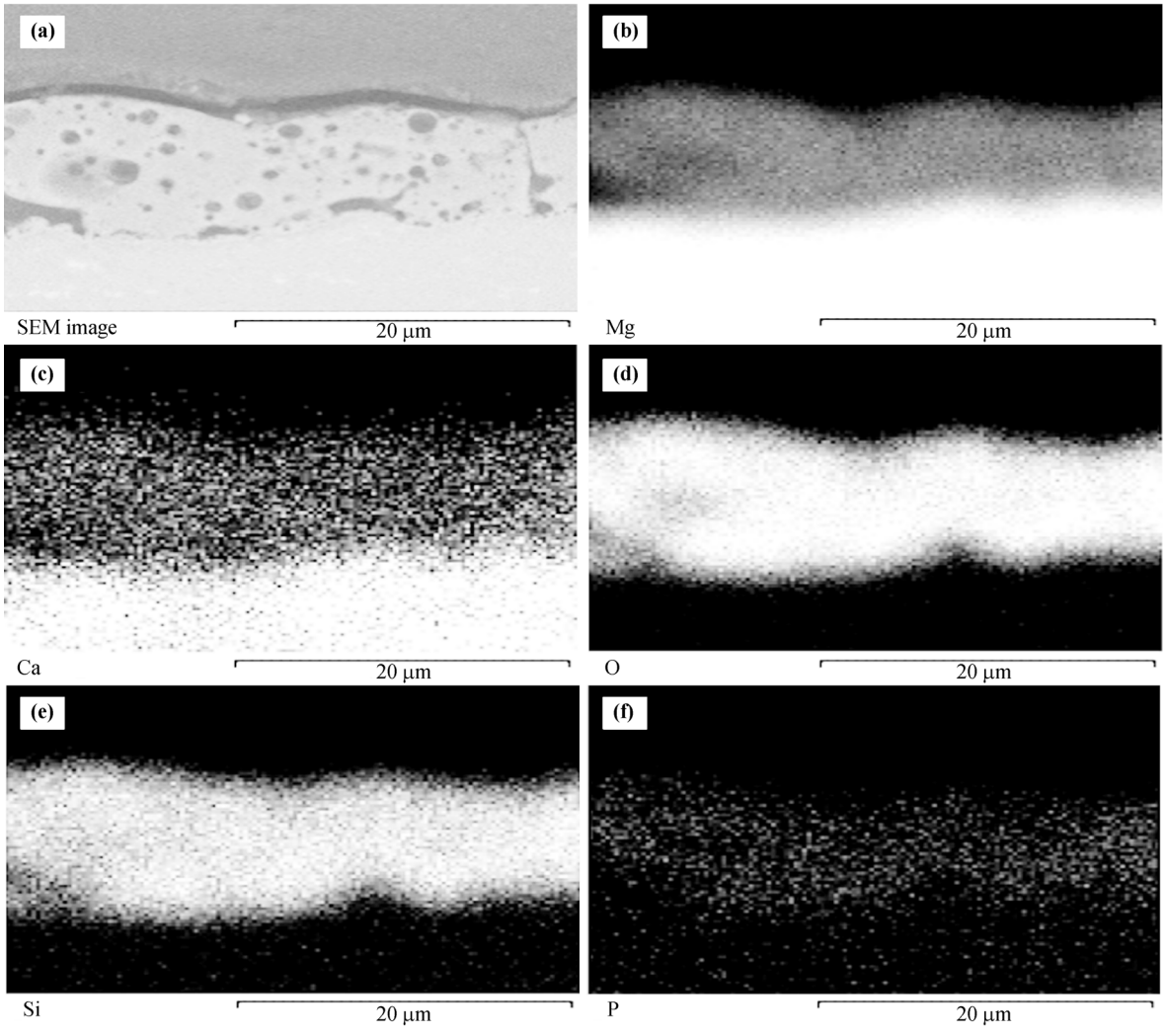

Fig. 3 Elemental mapping of **(a)** the MAO coating on cross-section: **(b)** Mg; **(c)** Ca; **(d)** O; **(e)** Si; **(f)** P.

protection for the substrate (Fig. 4). The corrosion current density for the substrate is 1.045×10^{-5} A/cm^2, while for the MAO coating and the MAO/PLA coating 6.313×10^{-6} and 1.702×10^{-6} A/cm^2, respectively. It is clear that the current density of the MAO/PLA coating was insignificantly reduced compared to the MAO coating due to the numerous microvoids in the PLA coating with a lower molecular weight.

The Nyquist plot (Fig. 5(a)) shows similar components: one capacitive reactance in high frequency range, a smaller capacitive reactance following in the middle frequency, and an inductance reactance arc in the low frequency range. The MAO and MAO/PLA coatings lead to an obvious improvement in the corrosion resistance in comparison to the substrate (Fig. 5).

There are two major capacitive reactances existing in the EIS curve of the MAO coating, which is in accordance with

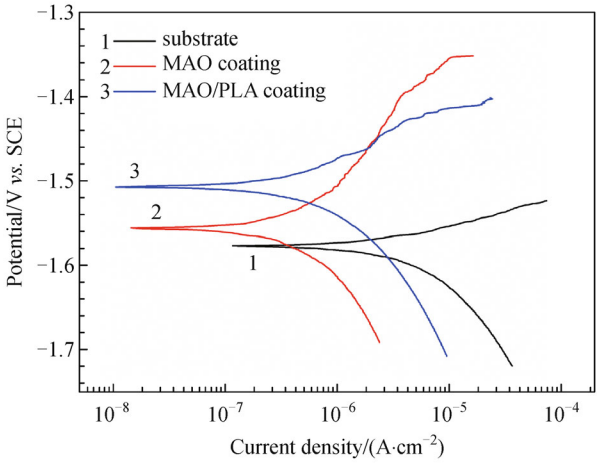

Fig. 4 Polarization curves of the substrate and its coatings in Hank's solution.

that of the MAO coatings reported in Refs. [20,35]. Polymer sealing slightly improved the corrosion resistance according to the Bode plot (Fig. 5(b)).

For the EIS of the substrate (Fig. 5), capacitive reactance arc in the high frequency (HF) region corresponds to electrical double layer at the interface of the solution and the substrate alloy; and capacitive reactance arc in the medium frequency (MF) region corresponds to oxidation layer formed in air; and the inductive reactance arc in the low frequency (LF) corresponds to the initiation of pitting corrosion. For the MAO and MAO/PLA coatings, capacitive reactance arc in the first HF region corresponds to the porous outer layer and the second arc corresponds to the denser barrier layer. Impedance reactance arc in LF region implies the absorption of products. The PLA coating cannot change the electrochemical corrosion characteristic of the composite coating because PLA still contains a high porosity (Figs. 1–2 and Table 1). The EIS plots were fitted by the equivalent circuit shown in Fig. 6. For the Mg substrate (Fig. 6(a)), R_s represents the solution resistance, R_{ct} represents the charge transfer resistance. Generally, the higher R_{ct} value implies the lower dissolution rate. The MAO coating improved R_{ct} obviously from 176.1 to 354.8 $\Omega \cdot cm^2$, while the PLA coating gave rise to 1894 $\Omega \cdot cm^2$. The R_f and C_f designate the second capacitive reactance arc in MF region. Constant phase element (CPE_f) is used to replace capacitance C_f in MAO coating. CPE_f indicates the deviation of C_f to theoretical value due to the considerably porous structure of MAO coating. A dimensionless coefficient, n was introduced to fix this deviation. Because the surface roughness of the composite coating was reduced by the PLA, n was removed. The second capacitive reactance arc is related to the denser sub-layer of the coating. The R_f value increases in the order: Mg substrate < MAO < MAO/PLA. The fitting results of EIS of the substrate and its coatings in Hank's solution are summarized in Table 2. The fitting quality was evaluated by the chi-squared values, which was the order of 10^{-4}, indicating that the obtained data was consistent with the proposed equivalent circuit [35].

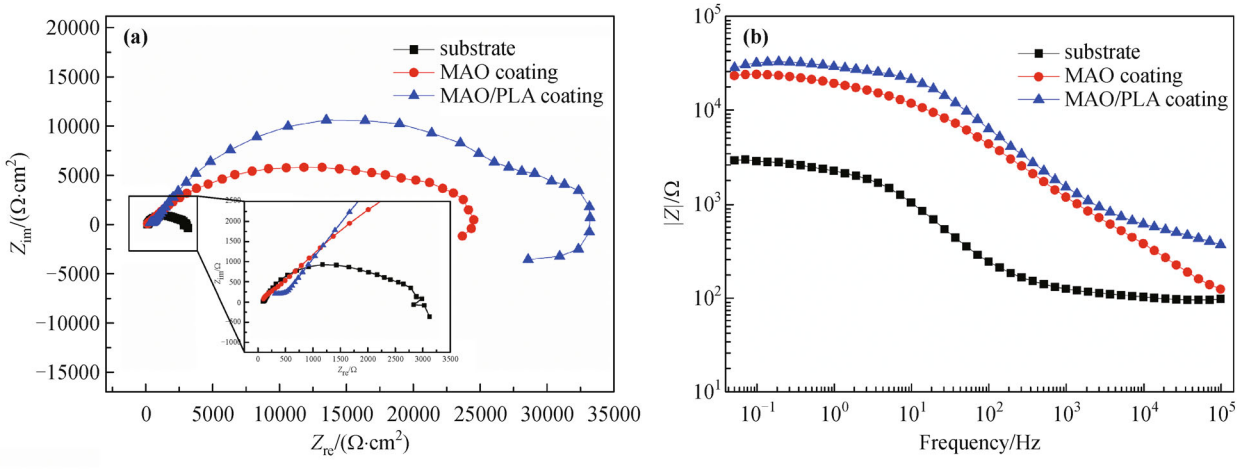

Fig. 5 **(a)** Nyquist plots and **(b)** Bode plots of the substrate and its coatings in Hank's solution.

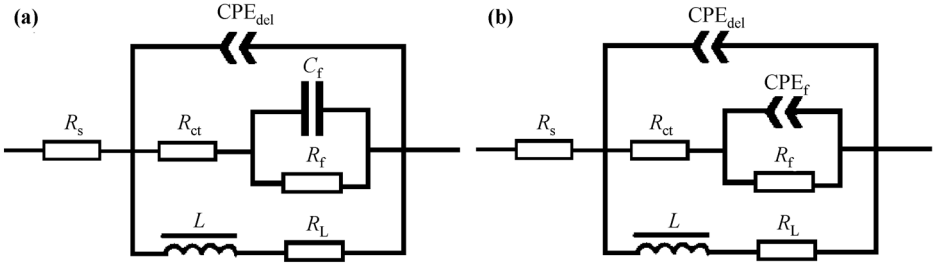

Fig. 6 Equivalent circuit of EIS: **(a)** the substrate and MAO/PLA composite coating; **(b)** the MAO coating in Hank's solution.

4 Discussion

4.1 Change in corrosion rate

The HER as a function of immersion time in Hank's solution is showed in Fig. 7. It is clear that the HER of the MAO/PLA coating was the lowest. The Mg–Li–Ca–Y substrate was subjected to attack and kept the HER at a high level at the beginning of soaking. While in the initial stage, the MAO coating showed a favorable corrosion resistance. However, as time increased, the HER of the MAO coating continuously accelerated. At the immersion time of 9 h, the HER of the MAO coating was almost equal to that of the substrate. And in the subsequent immersion, the HER of the MAO coating finally surpassed that of the substrate in Hank's solution. This scenario was out of the expectation. There was large discrepancy between the HER and the corrosion resistance obtained from the polarization curves and EIS. This was ascribed to the influence of the immersion time and thus the surface change in solutions. Particularly, the HER of the MAO coating surpassed that of its substrate in subsequent immersion. Further investigation on pH measurement was made to understand the corrosion mechanism of the coating. The immersion test merely lasted 30 h and demonstrated a preliminary comparison of corrosion rate; a long-term corrosion evaluation is needed in further research.

4.2 Change in pH value

The variation in pH value of the solution is a major concern for the applications of biomedical magnesium alloys. Thus, the change in pH values versus immersion time in Hank's solution was monitored (Fig. 8). It is noted that the pH value of the MAO coating was slightly lower than that of the substrate before 6 h, and vice versa after. This situation was similar to the change in HER.

At the first stage, the lower pH value of the MAO coating than the substrate was ascribed to the hydration of the ceramic oxide MgO by chemical reaction as follows:

$$MgO + H_2O \rightarrow Mg(OH)_2 \quad (1)$$

Simultaneously, the substrate was protected from the denser barrier layer against the solution, as illustrated in Fig. 9(a). The PBRs of MgO and $Mg(OH)_2$ are 0.8 and 1.80, respectively [17]. Therefore, the hydration of MgO led to an increase in volume of the precipitate of $Mg(OH)_2$. As a result, the pore of the MAO coating was partially sealed by the precipitate, which was partially protective.

Table 2 Fitting results of EIS of the substrate and its coatings in Hank's solution

Sample	R_s /($\Omega\cdot cm^2$)	Y_1 /($\Omega^{-1}\cdot cm^{-2}\cdot s^{-1}$)	n_1	R_{ct} /($\Omega\cdot cm^2$)	C_f /($F\cdot cm^{-2}$)	Y_2 /($\Omega^{-1}\cdot cm^{-2}\cdot s^{-1}$)	n_2	R_f /($10^4\Omega\cdot cm^2$)	L /($H\cdot cm^{-2}$)	R_L /($10^4\Omega\cdot cm^2$)	Chi-square /10^{-4}
Substrate	54.1	5.8×10^{-5}	0.7	176.1	2.3×10^{-6}	–	–	0.1	106.4	0.4	2.8
MAO	73.4	1.6×10^{-7}	0.9	354.8	–	5.6×10^{-6}	0.6	8.8	236.9	4.1	3.5
MAO/PLA	79.2	2.8×10^{-6}	0.7	1894.0	3.4×10^{-9}	–	–	9.5	559.9	5.6	7.4

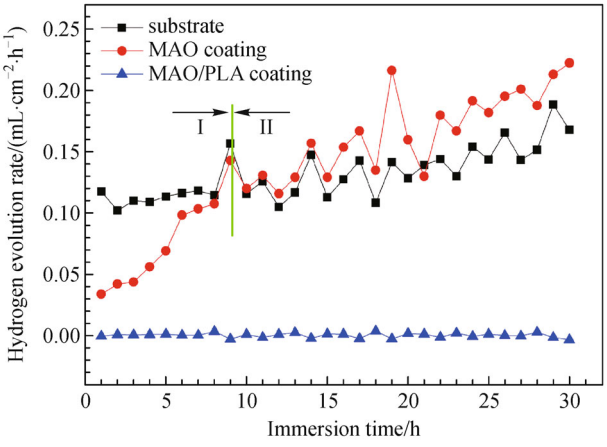

Fig. 7 HER of the substrate and its coatings in Hank's solution.

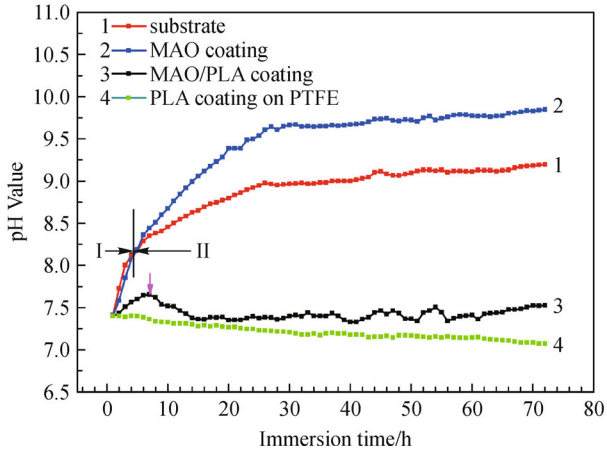

Fig. 8 Variation in pH values for the substrate and its coatings on the Mg–1.21Li–1.12Ca–1.0Y alloy and PLA coating on PTFE in Hank's solution.

Once the oxide transformed completely into $Mg(OH)_2$, then the solution would penetrate into the substrate.

At the second stage, the magnesium substrate was subjected to electrochemical corrosion from the aggressive medium, as represented in Fig. 9(b).

Anodic reaction

$$Mg \rightarrow Mg^{2+} + 2e^- \quad (2)$$

Cathodic reaction

$$2H_2O + 2e^- \rightarrow 2OH^- + H_2 \uparrow \quad (3)$$

Total reaction

$$Mg + 2H_2O \rightarrow Mg(OH)_2 + H_2 \uparrow \quad (4)$$

The hydrogen evolution would cause a continuous increase in pressure beneath the MAO coating and the $Mg(OH)_2$ precipitate with increasing time. However, the precipitate $Mg(OH)_2$ can be dissolved by chloride ions:

$$Mg(OH)_2 + 2Cl^- \rightarrow MgCl_2 + 2OH^- \quad (5)$$

Consequently, the partial MAO coating and dissolution of $Mg(OH)_2$ precipitate would break up and collapse under such a pressure that resulted in more areas exposed to the solution, and thus accelerated the corrosion of the MAO coating.

The linear decrease in solution pH for the PLA coating on the PTFE plate disclosed that the acidic products were developed during its degradation (Fig. 8). The pH result demonstrated that the acidification of the degradation of PLA neutralized the alkalinity of degradation of magnesium, and thus resulted in the pH value maintaining at a much lower level than the substrate. The slow rise in pH value (Fig. 8) for the MAO/coating in the initial immersion of 7 h was related to the fast absorbent feature of the porous PLA coating during its degradation and corrosion of magnesium. In the following period, the occurrence of the acidic resultants, resulting from the polymer degradation, gave rise to the decrease in pH value [36].

Figure 10 shows the cracked surface morphologies of

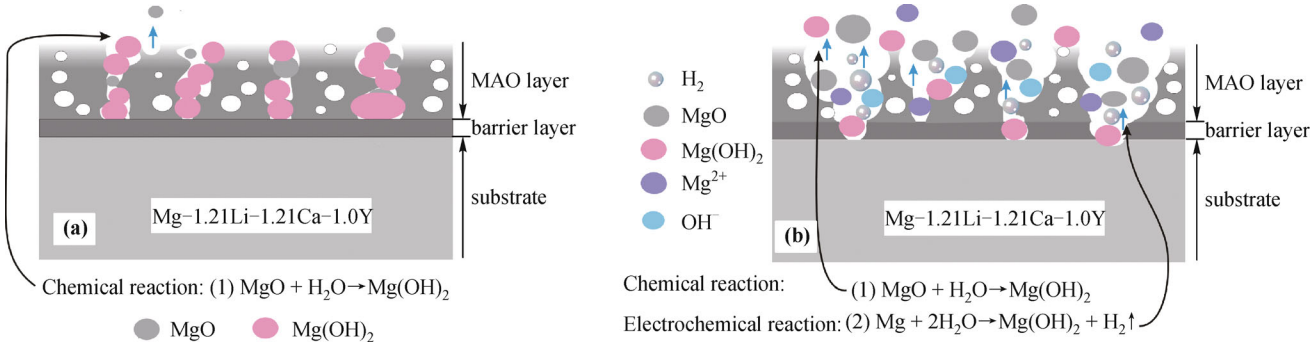

Fig. 9 Schematic illustration of the corrosion mechanism of the MAO coating: **(a)** at the first stage; **(b)** at the second stage.

MAO/PLA composite coating soaked in Hank's solution for 72 h. This morphology implies that the long chain of the polymeric coating degraded into short chain [27]. In the subsequent period, the PLA coating gently swelled and blocked the migration paths of water molecular and the ions into the MAO coating.

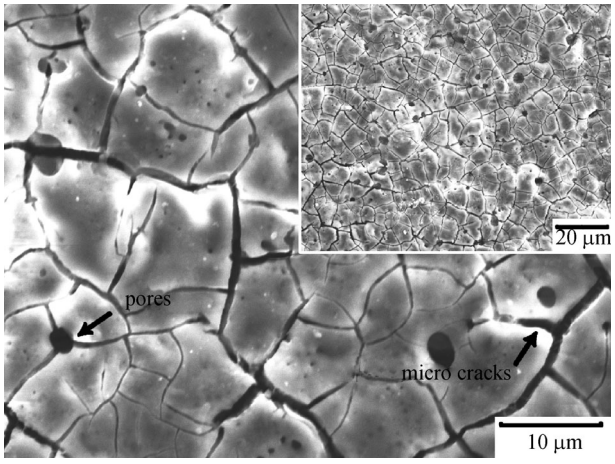

Fig. 10 SEM images of MAO/PLA coating soaked in Hank's solution for 72 h.

Figure 11 designates the XRD patterns of the MAO coating and the MAO/PLA composite coating soaked in Hank's solution for 72 h. There were no new phases formed besides the original components: MgO, Mg_2SiO_4, α-Mg, and Y_2O_3 in the MAO coating. The formation of the phases in the MAO coating can be attributable to the reactions through [37–38]:

$$Mg(OH)_2 \rightarrow MgO + H_2O \quad (6)$$

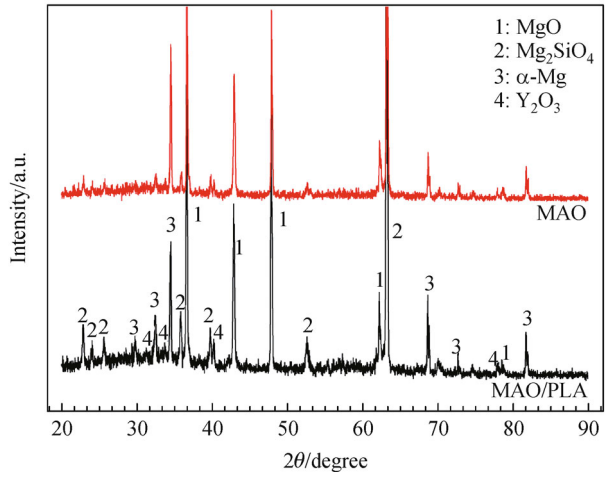

Fig. 11 XRD patterns of MAO and MAO/PLA coatings after immersion in Hank's solution for 72 h.

$$2Mg^{2+} + SiO_3^{2-} + 2OH^- \rightarrow Mg_2SiO_4 + H_2O \quad (7)$$

$$2Y^{3+} + 6OH^- \rightarrow 2Y(OH)_3 \rightarrow Y_2O_3 + 3H_2O \quad (8)$$

This result also verified the previous elemental analysis, even though the peaks of calcium phosphates were imperceptible because of lower content in MAO coating. The element enrichment of yttrium was conducive to improve corrosion resistance of MAO coating. The addition of phytic acid decreased the solution conductivity and increased the values of breakdown voltage [32]. The species of calcium phosphate could be $CaHPO_4$ or $Ca_3(PO_4)_2$ or amorphous calcium phosphate [21].

As a result, the pH value of the PLA-coated samples stabilized in the range from 7.5 to 7.8, which was fairly close to the ideal pH value in human body. Further comparison disclosed that the pH values of the MAO/PLA coating on Mg–Li–Ca–Y alloy was lower than the polymeric coating poly(L-lactic acid) (PLLA) on pure Mg (Fig. 8) [26]. This consequence also indicated the MAO/PLA coating has advantages over the pure polymeric coating.

5 Conclusions

1) The MAO coating on the Mg–1.21Li–1.12Ca–1.0Y alloy was characterized by MgO, Mg_2SiO_4, traces of Y_2O_3 and calcium phosphates.

2) The corrosion resistance of the Mg–1.21Li–1.12Ca–1.0Y alloy was markedly improved by MAO/PLA coating. The hydrogen evolution rate of the MAO-coated alloy accelerated gradually and surpassed that of the substrate after 6-h immersion, while that of the MAO/PLA coating remained at a lower value.

3) The MAO/PLA coating tailored the solution pH, which ranged from 7.5 to 7.8 in 3 d. This characteristic may prevent tissue subjected to the alkalization on the magnesium surface. The MAO/PLA coating may be a promising coating for biomedical Mg–1.21Li–1.12Ca–1.0Y alloys.

Abbreviations

CPE	constant phase element
EIS	electrochemical impedance spectroscopy
EMPA	electron microprobe analysis

HCP	hexagonal closed packed
HER	hydrogen evolution rate
HF	high frequency
LF	low frequency
MAO	micro-arc oxidation
MF	medium frequency
PBR	Pilling–Bedworth ratio
PCL	poly(ε-caprolactone)
PGA	poly(glycolic acid)
PLA	poly(lactic acid)
PLLA	poly(L-lactic acid)
PTFE	polytetrafluoroethylene
RE	rare earth element
SCE	saturated calomel electrode
SCM	single chip micyoco
SEM	scanning electron microscopy
XRD	X-ray diffraction

Acknowledgements This research was financially supported by the National Natural Science Foundation of China (Grant No. 51241001), Shandong Provincial Natural Science Foundation, China (ZR2011E MM004), SDUST Research Fund (2014TDJH104), Joint Innovative Center for Safe and Effective Mining Technology and Equipment of Coal Resources, and Shandong Province as well as Taishan Scholarship Project of Shandong Province (TS20110828). Thanks go to Prof. Rong-Shi Chen and the members of his group at Institute of Metals Research, Chinese Academy of Sciences for the preparation of the ingots.

References

[1] Staiger M P, Pietak A M, Huadmai J, et al. Magnesium and its alloys as orthopedic biomaterials: a review. Biomaterials, 2006, 27 (9): 1728–1734

[2] Zhao L, Cui C, Wang Q, et al. Growth characteristics and corrosion resistance of micro-arc oxidation coating on pure magnesium for biomedical applications. Corrosion Science, 2010, 52(7): 2228–2234

[3] Witte F, Fischer J, Nellesen J, et al. *In vitro* and *in vivo* corrosion measurements of magnesium alloys. Biomaterials, 2006, 27(7): 1013–1018

[4] Li Z, Gu X, Lou S, et al. The development of binary Mg–Ca alloys for use as biodegradable materials within bone. Biomaterials, 2008, 29(10): 1329–1344

[5] Song G, Song S. A possible biodegradable magnesium implant material. Advanced Engineering Materials, 2007, 9(4): 298–302

[6] Witte F. The history of biodegradable magnesium implants: a review. Acta Biomaterialia, 2010, 6(5): 1680–1692

[7] Gray J, Luan B. Protective coatings on magnesium and its alloys — a critical review. Journal of Alloys and Compounds, 2002, 336 (1–2): 88–113

[8] Xin Y, Hu T, Chu P K. *In vitro* studies of biomedical magnesium alloys in a simulated physiological environment: a review. Acta Biomaterialia, 2011, 7(4): 1452–1459

[9] Witte F, Kaese V, Haferkamp H, et al. *In vivo* corrosion of four magnesium alloys and the associated bone response. Biomaterials, 2005, 26(17): 3557–3563

[10] Liu C L, Wang Y J, Zeng R C, et al. *In vitro* corrosion degradation behaviour of Mg–Ca alloy in the presence of albumin. Corrosion Science, 2010, 52(10): 3341–3347

[11] Kim W C, Kim J G, Lee J Y, et al. Influence of Ca on the corrosion properties of magnesium for biomaterials. Materials Letters, 2008, 62(25): 4146–4148

[12] Zhang S, Li J, Song Y, et al. *In vitro* degradation, hemolysis and MC3T3-E1 cell adhesion of biodegradable Mg–Zn alloy. Materials Science and Engineering C, 2009, 29(6): 1907–1912

[13] Zhang C-Y, Zeng R-C, Liu C-L, et al. Comparison of calcium phosphate coatings on Mg–Al and Mg–Ca alloys and their corrosion behavior in Hank's solution. Surface and Coatings Technology, 2010, 204(21–22): 3636–3640

[14] Zhang C Y, Zeng R C, Chen R S, et al. Preparation of calcium phosphate coatings on Mg–1.0Ca alloy. Transactions of Nonferrous Metals Society of China, 2010, 20: s655–s659

[15] Zeng R C, Dietzel W, Witte F, et al. Progress and challenge for magnesium alloys as biomaterials. Advanced Engineering Materials, 2008, 10(8): B3–B14

[16] Zeng R C, Guo X L, Liu C L, et al. Study on corrosion of medical Mg–Ca and Mg–Li–Ca alloys. Acta Metallurgica Sinica, 2012, 47: 1477–1482

[17] Zeng R C, Sun L, Zheng Y F, et al. Corrosion and characterisation of dual phase Mg–Li–Ca alloy in Hank's solution: The influence of microstructural features. Corrosion Science, 2014, 79: 69–82

[18] Witte F, Fischer J, Nellesen J, et al. *In vitro* corrosion and corrosion protection of magnesium alloy LAE442. Acta Biomaterialia, 2010, 6(5): 1792–1799

[19] Zhao X, Shi L L, Xu J. A comparison of corrosion behavior in saline environment: rare earth metals (Y, Nd, Gd, Dy) for alloying of biodegradable magnesium alloys. Journal of Materials Science and Technology, 2013, 29(9): 781–787

[20] Chen J, Zeng R C, Huang W J, et al. Characterization and wear resistance of macro-arc oxidation coating on magnesium alloy AZ91 in simulated body fluids. Transactions of Nonferrous Metals Society of China, 2008, 18: s361–s364

[21] Sankara Narayanan T S N, Park I S, Lee M H. Strategies to improve the corrosion resistance of microarc oxidation (MAO) coated magnesium alloys for degradable implants: Prospects and challenges. Progress in Materials Science, 2014, 60: 1–71

[22] Xu L, Pan F, Yu G, et al. *In vitro* and *in vivo* evaluation of the surface bioactivity of a calcium phosphate coated magnesium alloy. Biomaterials, 2009, 30(8): 1512–1523

[23] Xu L, Yamamoto A. *In vitro* degradation of biodegradable polymer-coated magnesium under cell culture condition. Applied Surface Science, 2012, 258(17): 6353–6358

[24] Hornberger H, Virtanen S, Boccaccini A R. Biomedical coatings on magnesium alloys — a review. Acta Biomaterialia, 2012, 8(7): 2442–2455

[25] Gu X N, Li N, Zhou W R, et al. Corrosion resistance and surface biocompatibility of a microarc oxidation coating on an Mg–Ca alloy. Acta Biomaterialia, 2011, 7(4): 1880–1889

[26] Xu L, Yamamoto A. Characteristics and cytocompatibility of biodegradable polymer film on magnesium by spin coating. Colloids and Surfaces B: Biointerfaces, 2012, 93: 67–74

[27] Wu Y H, Li N, Cheng Y, et al. *In vitro* study on biodegradable AZ31 magnesium alloy fibers reinforced PLGA composite. Journal of Materials Science and Technology, 2013, 29(6): 545–550

[28] Wong H M, Yeung K W, Lam K O, et al. A biodegradable polymer-based coating to control the performance of magnesium alloy orthopaedic implants. Biomaterials, 2010, 31(8): 2084–2096

[29] Ostrowski N J, Lee B, Roy A, et al. Biodegradable poly(lactide-co-glycolide) coatings on magnesium alloys for orthopedic applications. Journal of Materials Science: Materials in Medicine, 2013, 24(1): 85–96

[30] Guo M, Cao L, Lu P, et al. Anticorrosion and cytocompatibility behavior of MAO/PLLA modified magnesium alloy WE42. Journal of Materials Science: Materials in Medicine, 2011, 22 (7): 1735–1740

[31] Lu P, Cao L, Liu Y, et al. Evaluation of magnesium ions release, biocorrosion, and hemocompatibility of MAO/PLLA-modified magnesium alloy WE42. Journal of Biomedical Materials Research Part B: Applied Biomaterials, 2011, 96B(1): 101–109

[32] Zhang R F, Zhang S F, Duo S W. Influence of phytic acid concentration on coating properties obtained by MAO treatment on magnesium alloys. Applied Surface Science, 2009, 255(18): 7893–7897

[33] Gaurava S, Ankita M, Pradeep S. Characterization and *in vitro* degradation studies of synthesized polylactide (PLA). Research Journal of Chemistry and Environment, 2012, 16: 2

[34] Bonilla F, Berkani A, Skeldon P, et al. Enrichment of alloying elements in anodized magnesium alloys. Corrosion Science, 2002, 44(9): 1941–1948

[35] Sreekanth D, Rameshbabu N, Venkateswarlu K, et al. Effect of K_2TiF_6 and $Na_2B_4O_7$ as electrolyte additives on pore morphology and corrosion properties of plasma electrolytic oxidation coatings on ZM21 magnesium alloy. Surface and Coatings Technology, 2013, 222: 31–37

[36] Piemonte V, Gironi F. Kinetics of hydrolytic degradation of PLA. Journal of Polymers and the Environment, 2013, 21(2): 313–318

[37] Ghasemi A, Raja V S, Blawert C, et al. The role of anions in the formation and corrosion resistance of the plasma electrolytic oxidation coatings. Surface and Coatings Technology, 2010, 204 (9–10): 1469–1478

[38] Wang L, Pan C. Characterisation of microdischarge evolution and coating morphology transition in plasma electrolytic oxidation of magnesium alloy. Surface Engineering, 2007, 23(5): 324–328